the plant journal

SEB Society for Experimental Biology

The Plant Journal (2019) **99,** 316–328 doi: 10.1111/tpj.14326

Comprehensive phenotyping reveals interactions and functions of *Arabidopsis thaliana* TCP genes in yield determination

Sam W. van Es[1,2,†], Elwin B. van der Auweraert[1], Sylvia R. Silveira[1,3], Gerco C. Angenent[1,2], Aalt D.J. van Dijk[4,5] and Richard G.H. Immink[1,2,*]

[1]*Bioscience, Wageningen Plant Research, Wageningen University and Research, 6708 PB, Wageningen, The Netherlands,*
[2]*Laboratory of Molecular Biology, Wageningen University and Research, 6708 PB, Wageningen, The Netherlands,*
[3]*Laboratório de Biotecnologia Vegetal, Centro de Energia Nuclear na Agricultura, Universidade de São Paulo, Piracicaba, SP, CEP 13416-000, Brazil,*
[4]*Biometris, Wageningen University and Research, 6708 PB, Wageningen, The Netherlands, and*
[5]*Bioinformatics, Wageningen University and Research, 6708 PB, Wageningen, The Netherlands*

Received 8 January 2019; revised 6 March 2019; accepted 15 March 2019; published online 22 March 2019.
*For correspondence (e-mail richard.immink@wur.nl).
[†]Present address: Department of Plant Physiology, Umeå Plant Science Centre, Umeå University, 90187 Umeå, Sweden.

SUMMARY

Members of the *Arabidopsis thaliana* TCP transcription factor (TF) family affect plant growth and development. We systematically quantified the effect of mutagenizing single or multiple TCP TFs and how altered vegetative growth or branching influences final seed yield. We monitored rosette growth over time and branching patterns and seed yield characteristics at the end of the lifecycle. Subsequently, an approach was developed to disentangle vegetative growth and to determine possible effects on seed yield. Analysis of growth parameters showed all investigated tcp mutants to be affected in certain growth aspects compared with wild-type plants, highlighting the importance of TCP TFs in plant development. Furthermore, we found evidence that all class II TCPs are involved in axillary branch outgrowth, either as inhibitors (BRANCHED-like genes) or enhancers (JAW- and TCP5-like genes). Comprehensive phenotyping of plants mutant for single or multiple TCP TFs reveals that the proposed opposite functions of class I and class II TCPs in plant growth needs revision and shows complex interactions between closely related TCP genes instead of full genetic redundancy. In various instances, the alterations in vegetative growth or in branching patterns result into negative trade-off effects on seed yield that were missed in previous studies, showing the importance of comprehensive and quantitative phenotyping.

Keywords: TCP transcription factor, plant growth, yield, phenotyping, *Arabidopsis thaliana*, plant architecture.

INTRODUCTION

The major challenge of modern agriculture is to produce increasing amounts of high quality biomass for food, feed, and bio-based products, with a minimal ecological footprint. Final yield, in the form of seeds, fruits, or leaves (e.g. leafy vegetables), depends strongly on plant architecture, organ size, and tissue longevity (Busov *et al.*, 2008; Cai *et al.*, 2016). Therefore, these traits have been the subject of breeding since the dawn of agriculture.

Our research aims at identifying genes involved in the control of plant development and architecture and finding possible correlations between their functioning and yield characteristics. We focus on key regulatory factors belonging to the TCP TF family in the plant model species *Arabidopsis thaliana*. Genes of this family orchestrate numerous growth-related processes during Arabidopsis development (for review see Uberti Manassero *et al.*, 2013). The TCP family consists of two classes with supposed opposite function; TCPs of class I are thought to be activators of growth and genes in class II to act as growth suppressors (Li *et al.*, 2005). Examples in Arabidopsis include the role of *BRANCHED1* (*BRC1*) and *BRC2* in the outgrowth of axillary branches (Aguilar-Martínez *et al.*, 2007), determination of leaf shape and curvature by *JAW-TCPs* (Nath *et al.*, 2003; Palatnik *et al.*, 2003) and effects on

leaf size by *TCP5-like* genes (Efroni *et al.*, 2008). Nevertheless, for one of the founding members of TCPs, *CYCLOIDIA* (*CYC*) in *Antirrhinum majus*, both growth activating and repressing functions were found, depending on the developmental stage and cellular context (Luo *et al.*, 1995), revealing lack of complete linkage between TCP classification and function.

TCP gene functions appear to be conserved between species and a mutation in the maize *TEOSINTE BRANCHED1* (*TB1*) *locus*, the orthologue of Arabidopsis *BRANCHED*-like genes, resulted in an higher expression and increased apical dominance, which has been instrumental in the domestication of maize from its ancestor teosinte (Doebley *et al.*, 1995, 1997). Branching phenotypes have been observed as well in rice plants with a mutation in the *TB1*-like gene (Takeda *et al.*, 2003). The *JAW*-TCPs (*TCP2*, *-3*, *-4*, *-10*, and *-24*) are simultaneously targeted by a microRNA (miR319) in Arabidopsis. Overexpression of miR319 leads to the *jaw-D* mutant, which has a striking crinkled leaf phenotype due to an overproduction of cells in the leaf margins (Nath *et al.*, 2003; Palatnik *et al.*, 2003; Efroni *et al.*, 2008). Similarly, tomato miR319 is required for normal leaf development by regulating the tomato JAW-TCP homologue *LANCEOLATE* (Ori *et al.*, 2007).

The above-mentioned examples indicate the importance of the TCP TF family for the regulation of growth and plant architecture in the model species Arabidopsis and various crops. The more detailed our knowledge on the specific function of these TCPs and their potential combined effects on plant development, the more we will be able to precisely direct breeding for yield optimization by altering for example leaf growth and branching patterns (tillering).

Even though many reports about individual members of the TCP family of TFs are available (reviewed by Danisman, 2016), a comprehensive and detailed phenotyping of the various single and combined *tcp* gene mutants is lacking. This analysis is essential to understanding the role and importance of each individual *TCP* gene, the genetic interactions between the different *TCP* genes, and how effects on one trait influence other traits and/or final yield parameters. Most phenotypes observed so far consist of snapshots at a given time point, specific stage or on specific tissues or organs. This inevitably limits the documentation of phenotypes, which occur in a dynamic manner. Furthermore, it does not allow for an analysis on how phenotypes, such as leaf size and final seed yield, might be linked.

One of the difficulties of studying genes affecting growth and growth speed is that phenotypes are often only noticeable when careful measurements are performed. For example, an increase in leaf surface area of five percent is very difficult to identify with the naked eye, while it could give rise to a substantial increase in biomass production. Furthermore, it is evident that mutations resulting in altered developmental progression, such as *tcp* mutants affecting leaf growth rate, can be recorded only if a temporal component is included in the analysis (Boyes *et al.*, 2001). Plants mutated for *TCP20* for instance, show an increase in leaf pavement cell size in young developing leaves, whereas no difference in final leaf size could be detected (Danisman *et al.*, 2012).

Functional redundancy has been shown and suggested for various members of the TCP family (Cubas *et al.*, 1999; Danisman *et al.*, 2013). For example, a single knockout of a gene of the Arabidopsis *CIN-TCP* clade produces only mild phenotypes, whereas knocking-down the whole clade shows dramatic changes in leaf development (Palatnik *et al.*, 2003; Schommer *et al.*, 2008). In this study, we analysed a well defined set of single and combined *tcp* mutants for several growth and yield parameters. Analysing various combinations of mutants (e.g. single, double, and triple) enables further analyses of the proposed functional redundancy within the TCP family and to decipher the contribution of individual TCPs to specific growth and development related functions.

In this study, temporal phenotyping analyses were performed using the 'Phenovator' platform (Flood *et al.*, 2016). Using this phenotyping platform, all the above-mentioned traits and characteristics were monitored in various *tcp* mutant lines and compared with wild-type plants. The plants were imaged during the vegetative developmental stage at several moments of the day, allowing the measurement of rosette size, growth rate, and photosynthetic efficiency. Phenotyping of the branching traits, yield, and seed characteristics was performed on the matured and full-grown plants. We converted the data on growth and development into an equation representing growth over time and coupled these results to other phenotypic parameters. This provided insights into the function of several members of the TCP TF family, as well as on the presumed redundancy of several TCPs. For all the genotypes studied, a difference in at least one of the growth equation parameters was observed, seemingly unlinked to which class (I or II) of TCP TFs the respective mutant belongs. The latter questions the validity of the historical functional division of the TCP family of TFs based on sequence similarity. Our phenotypic analysis revealed that there is no example showing absolute redundancy among related genes from a subclass of *TCPs* and their growth phenotypes. Furthermore, we showed that, under our growing conditions, an alteration in branching pattern (regardless of an increase or decrease in number of branches), leads to a decrease in final yield. Lastly, we hypothesised that all class II TCPs influence branching architecture of a plant grown with a higher plant density, possibly through involvement in light-sensing.

RESULTS

Mutant selection

The full set of *tcp* mutants that was analysed for developmental, architectural, and yield parameters can be found in Table S1(a). This set was further classified into subgroups using defined sequence and function-associated characteristics. The family of TCP transcription factors has been divided into two classes based on differences in their TCP domains (Cubas *et al.*, 1999). The second class of TCPs (Class II) can be subdivided into the groups CYC/TB1 (*BRANCHED*-likes) and CIN based on sequence homology. For all these class II TCP genes biological functions have been assigned based on their respective mutant phenotypes (Alonso *et al.*, 2003; Palatnik *et al.*, 2003; Aguilar-Martínez *et al.*, 2007; Efroni *et al.*, 2008; van Es *et al.*, 2018). Sequence-based subdivision of class I TCPs is less profound and slightly different parameters in phylogeny studies yield rather different phylogenetic trees (Martín-Trillo and Cubas, 2010; Aguilar-Martínez and Sinha, 2013; Danisman *et al.*, 2013; Danisman, 2016). It is therefore difficult to determine subgroups and to predict potential functional redundancy among class I TCPs, solely based on sequence information. An interesting approach was taken by Danisman *et al.* (2013), who combined sequence similarity, gene expression patterns, and protein−protein interaction capacity to predict functional redundancy and to classify members of the Arabidopsis *TCP* family. With that knowledge in mind, we created two subgroups of class I TCPs: '*TCP20*-likes' and '*TCP15*-likes'. In addition, we created the group '*TCP20*-associated', for which the selection criteria included information on downstream targets of TCP20 (Danisman *et al.*, 2012), besides the redundancy prediction (Danisman *et al.*, 2013).

Several of the selected *tcp* mutants have strong developmental phenotypes and were used for validation of the approach and critical evaluation of the followed methodology. An example is the *jaw-D* mutant, which is known to exhibit slowly developing leaves that eventually grow larger than leaves of wild-type plants (Efroni *et al.*, 2008). Obvious candidates to study the relation between branching and yield are the mutants in the *BRANCHED-like* TCPs (Aguilar-Martínez *et al.*, 2007). Additionally, we focused on the analysis of potential functional redundancy within the TCP TF family, and included among others the double mutant *tcp14tcp15* (Kieffer *et al.*, 2011), *tcp8tcp15*, as well as the single *tcp8* and *tcp15* mutants (group '*TCP15*-likes').

Experimental set-up and technical constrains of the 'Phenovator' platform

The Phenovator platform (Flood *et al.*, 2016) allows the growth of 1440 plants simultaneously in a grid of 24 by 60 plants (Figure S1a). This grid was divided into 28 plots in which all 24 selected genotypes (Table S1a) were randomly positioned to allow for the correction of a possible positional bias. A regression analysis was performed to check for a possible effect of the plant's position in the growth chamber. The average size of all plants over time, as well as the maximum size was plotted on the X- and Y-coordinates corresponding to their position in the growth chamber (Figure S1a). We found a correlation between the X-coordinate and both maximum and average growth for our plants (Figure S1b). No significant correlation between Y-coordinate and projected leaf area (PLA) was detected (Figure S1c). The R-package SpATS (Rodríguez-Álvarez *et al.*, 2016; Velazco *et al.*, 2017) was used to correct for the observed spatial effect in the X-position. Although the growth chamber is expected to have near identical conditions regardless of the position within the chamber, the observed positional effect in the X-direction might be due to small differences in for example air flow, humidity or nutrient availability. The latter mentioned effects could be introduced due to the inflow of water with nutrients from one side of the chamber ($X \approx 0$; Figure S1a).

Arabidopsis rosette development follows an S-curve that includes an oscillatory component

Plant growth consists of two opposing factors: the intrinsic tendency toward unlimited increase (exponential growth phase) and restraints imposed by environmental resistance and ageing (resulting in an asymptotic maximum area) (Zeide, 1993). These two factors result in an S-curve growth function (Tessmer *et al.*, 2013). Furthermore, plant leaves move rhythmically up and down in a circadian fashion (Engelmann *et al.*, 1992). Singular spectrum analysis (SPA) on the PLA confirmed that the progress of Arabidopsis rosette growth contains two parts, an S-curve and an oscillatory function (Figure S2a).

An essential part in analysing plant size in a time series is to convert the data into an equation representing growth over time. Creating a growth-curve equation fitting the observed data enables turning different sizes and growth speeds into easily distinguishable parameters. The near-infrared (NIR) data were used to determine PLA as the latter provides a good estimate of above-ground biomass (Leister *et al.*, 1999) and can therefore be used to determine plant growth. This provides insight into growth dynamics of all mutant lines over time and enables a step beyond investigating average final plant sizes only.

The S-curve (Figure S2b) contains parameters that account for the distance between the two asymptotes (β_1), that describe the magnitude of the derivative (β_2), and the point at which the derivative of the function reaches its maximum (β_3). Next, the function to describe the circadian rhythm is an oscillatory function (Figure S2c) with certain amplitude (β_4) and phase (β_5). These two functions combined allowed us to determine the actual growth function (1). With the described combination of starting values and

bounds for the parameters (see Experimental procedures), the algorithm converges for all the time series and the values for β_1–β_5 could be determined. An example of a fitted function is shown in Figure S2(d). The obtained β-values allow us to look at the growth function in more detail and to extract the most likely biological meaning of the different β-parameters. For instance, the parameter β_1 could represent the maximum possible growth; β_2 a measure for the rate of growth in the exponential phase and β_3 a measure for the time until the rosette of a plant starts its rapid growth phase. β_4 is the change in measured rosette area relative to the real rosette area at that moment as a result of oscillatory leaf movement and β_5 is the starting point of this oscillation related to the circadian rhythm.

Growth parameter analyses

The nature of the measurements enables measurement of the rosette surface area, but not distinguishing individual leaves and their shape and size. Although the β-values in the growth equation described above cannot be directly linked to a particular growth parameter, we used a careful interpretation to disassemble the dynamic growth at plant level. Average β-values and their standard deviation per plant line were plotted (Figure S3a) and the parameters β_2 and β_3 were scaled to the lowest value to enhance readability of the graph. Statistical tests show differences in β-values comparing the mutant lines with wild-type control plants (Figure S3b). In short, all *tcp* mutants studied show alterations in developmental progress compared with wild-type control plants. Subsequently, a principal component analysis (PCA) was performed to visualise potential differences for the various *tcp* mutants (Figure 1).

A group of class I TCPs more closely studied on a cellular level and for possible redundancy are the *TCP20*-likes and *TCP20*-associated (Danisman *et al.*, 2012, 2013; Table S1a). Cells in leaves of several of these mutants are shown to enter the elongation phase earlier than leaf cells of wild-type control plants. In line with this, we found that *tcp19tcp20tcp22*, *tcp9*, and *tcp20* exhibit a lower β_3 than wild-type control. Contrastingly, the double *tcp9tcp20* mutant does not show a difference in β_3 compared with wild-type.

The other class I TCPs studied here, the *TCP15*-likes, are characterised by a higher β_1 and β_3, with *tcp8tcp15* as notable exception, having only a lower β_1 compared with wild-type control plants. The latter could indicate that the combination of *tcp8* and *tcp15* single mutations attenuates their individual growth and development effects.

A clear example of a class II mutant with altered development is the *jaw-D* mutant, shown to have a significantly lower β_2 but higher β_3. This represents the plants' characteristic and well known slow developmental progress (Palatnik *et al.*, 2003) through slow growth rate (β_2) and longer time to reach the rapid growth phase (β_3). Together with the *tcp5tcp13tcp17* triple mutant, *jaw-D* is the only mutant that has a lower β_2 compared with the wild-type, as visualized by the PCA plots in Figure 1. By contrast, *tcp10* has a higher β_1 than wild-type, i.e. a larger final size, fitting earlier research (Schommer *et al.*, 2008). At a cellular level, β_2 might be linked to the speed of cell elongation, fitting with the observed growth phenotypes of the *jaw-D* and the *tcp5tcp13tcp17* triple mutant.

The *tcp5* single mutant shows a phenotype opposite of that of the triple *tcp5tcp13tcp17* mutant as it has a significant higher β_1 and β_3. The mutant overexpressing *TCP5* in the epidermis only (*pATML1:TCP5*; van Es *et al.*, 2018) shows a higher β_2 and β_3. Overexpressing *TCP13* in a similar manner results in a higher β_1 and a lower β_3.

Members of the *BRANCHED*-like group of TCPs are best known for their role in branching. Next to altered branching patterns, plants mutated for these genes show an altered developmental progression of plant growth. Plants of the *brc1brc2* double mutant reach their maximum growth faster (β_3) and have a significantly smaller final size (β_1) than the wild-type control plants. Interestingly, the single mutants *brc1* and *brc2* show opposite behavior compared with the double *brc1brc2* mutant concerning β_1 and deviate from the double in that *brc1* has a higher β_3 value, whereas *brc2* appears to have a higher growth speed (β_2).

It must be noted that our interpretation of the final size of a plant is influenced by the duration of the measurements, i.e. some plants might not have reached full size by the time the PLA measurements had stopped. Another way to visualise growth is by plotting the PLA over time for the raw data versus the model (Figure 2a), showing their resemblance. This was followed by plotting the raw data for the *brc* mutants and Col-0 control in Figure 2(b), revealing the lower β_1 for the *brc1brc2* mutant for example. Figure 2(b) shows that the higher growth speed (β_2) might have led to the overall bigger *brc2* plant, whereas *brc1* only 'catches up' later, having reached its maximum growth speed (β_3) faster.

Photosynthetic capacity of plants

Next to size measurements based on PLA, the 'Phenovator' camera is monitoring photosynthetic efficiency of the plants under study. For this purpose, the system uses pulse amplitude modulated (PAM) chlorophyll fluorescence imaging to measure the light-use efficiency of PSII electron transport (ΦPSII) (Genty *et al.*, 1989; Baker, 2008; Flood *et al.*, 2016). Based on the average output of the ΦPSII measurement for all wild-type and *tcp* mutant lines, no significant differences were found (Figure S4), revealing that none of the analysed *TCP* transcription factors was having a direct effect on photosynthetic efficiency during the investigated timespan of plant development.

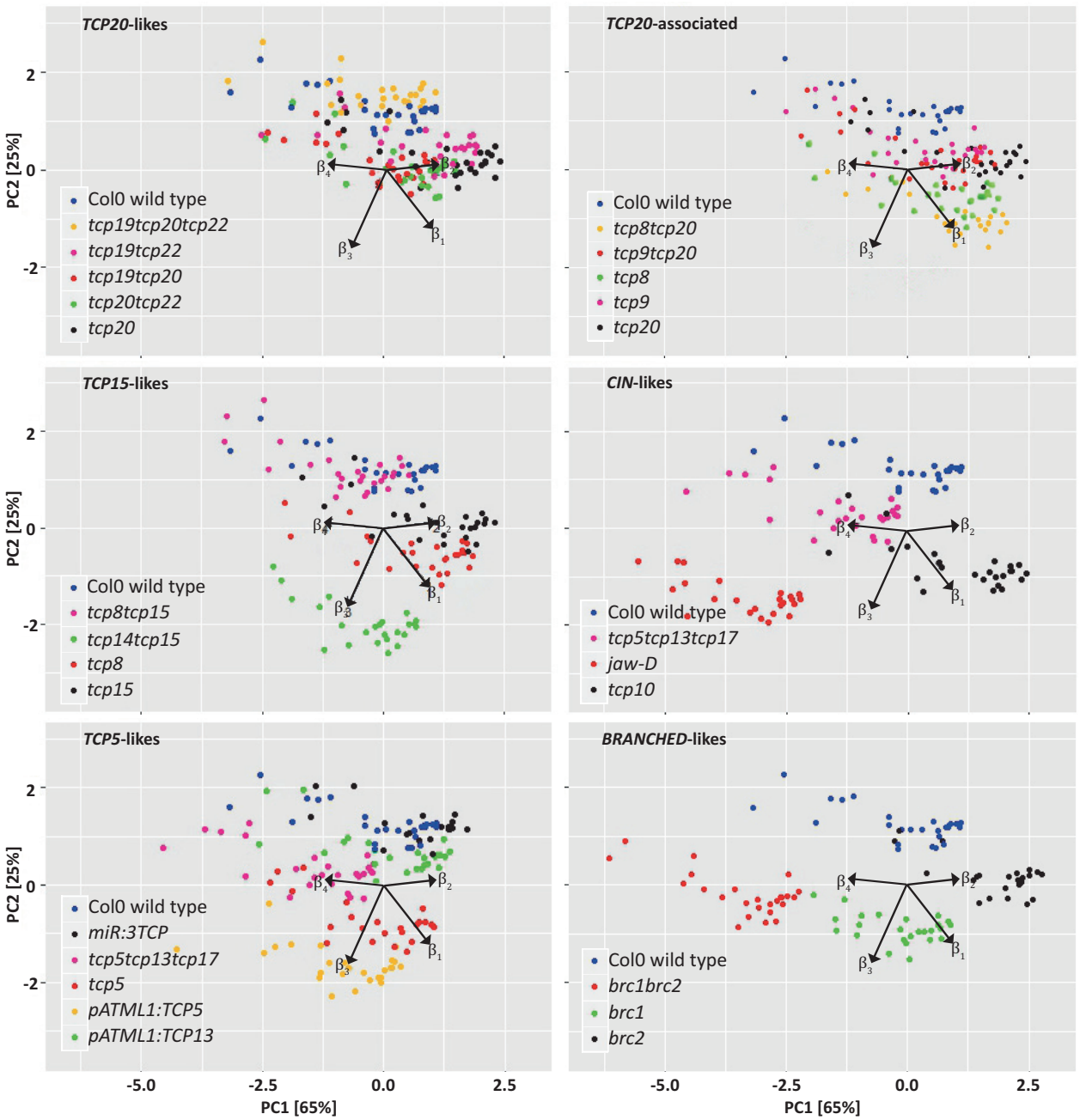

Figure 1. Principal component analysis (PCA) plots for individual β-values of all lines in this study. Results of a PCA for all the βs to examine a possible difference in mutants versus wild-type. For visual clarity the plots are made up for selected subgroups of *tcp* mutants, always including the Col0 wild-type as the control. Each data point in the PCA plot represents an individual plant. The β_1, β_2, β_3 and β_4 variable loadings are depicted as arrows. Combined, principal components 1 and 2 explain 90% of all variance (PC1 explains 65% of the variation, PC2 explains 25%).

Seed yield characteristics

Several characteristics of seeds were determined. Final yield was measured by weighing all the seeds for eight plants per genotype. Seed characteristics were explored in more detail by measuring seed size and seed number per silique on four siliques of five plants per genotype. We found that average seed size was not significantly affected in any of the analysed mutants (Figure 3a), whereas several lines showed a reduction in the average number of seeds per silique and total seed weight (Figure 3b,c). Only the seeds of the double mutant *tcp8tcp15* were significantly lighter compared with wild-type seeds (Figure 3d). Correlation analyses of the different seed characteristics revealed that the

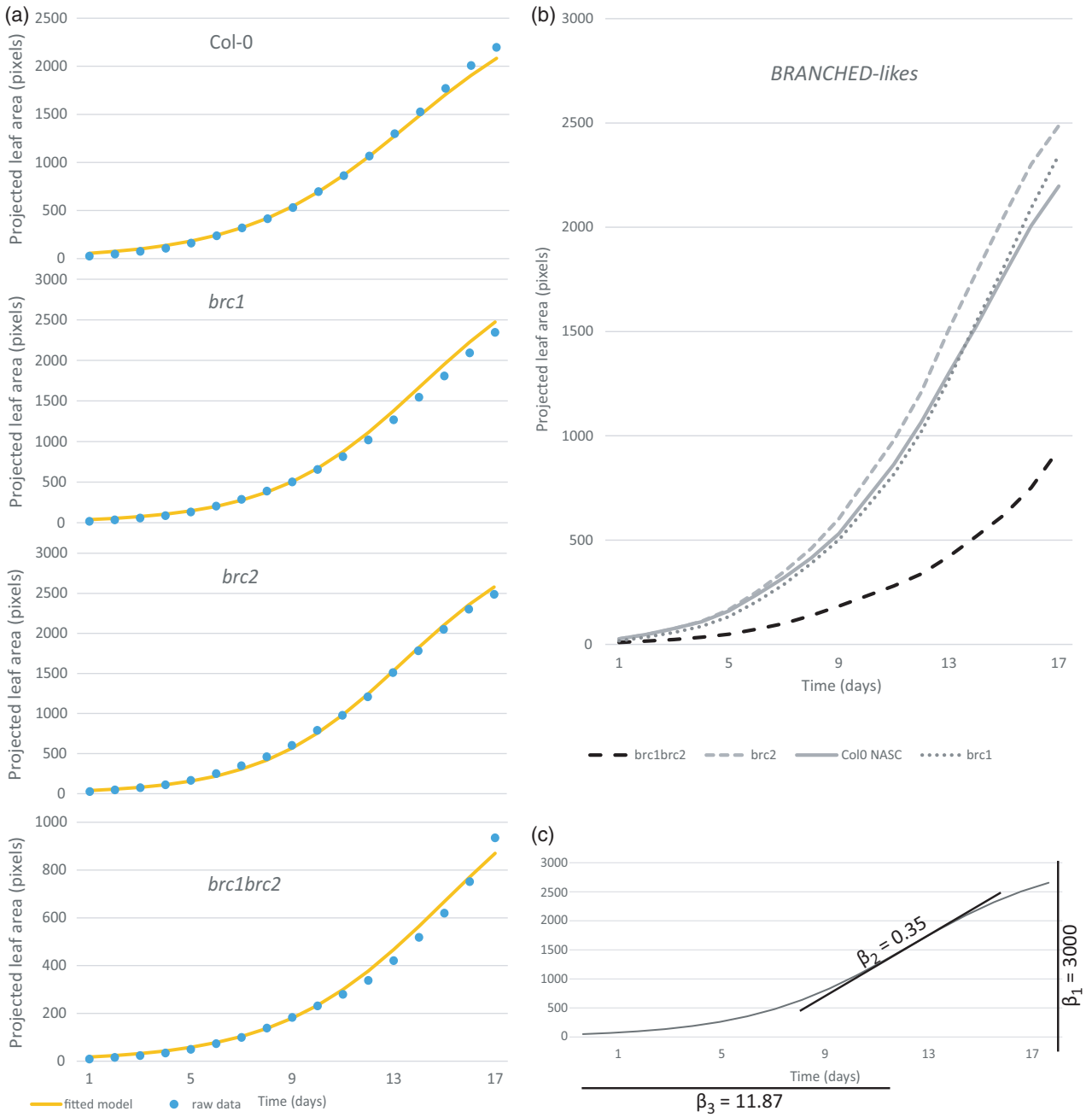

Figure 2. Visualisation of model versus raw data of *BRANCHED* TCPs.
(a) Shows the fitted model (yellow line) and the raw data (blue data points) for four plant lines during the 17 days of measurement. A comparison of the fitted model of the three branched mutants and a wild-type control (b) showing the different growth curves. An example of a fitted S-curve for three β-values shown in (c). Shown in (a) and (b) is the average projected leaf area per plant for each line, with measurements from one time point during the day, omitting the circadian rhythm for visual clarity.

number of seeds is negatively correlated with both seed area and seed weight and that seed weight is positively correlated with seed area (Figure S5a–c). Several lines showed a decrease in total seed weight (i.e. total yield), such as the *brc1brc2* double mutant and *jaw-d*, but also two *tcp15*-related double mutants: *tcp8tcp15* and *tcp14tcp15*.

TCPs affecting branching parameters; old acquaintances and new friends

To obtain insight in the effects of mutating or modifying expression levels of particular TCPs on plant architecture, the number and type of branches were quantified for all lines studied. In Figure 4(b), data on all the lines that

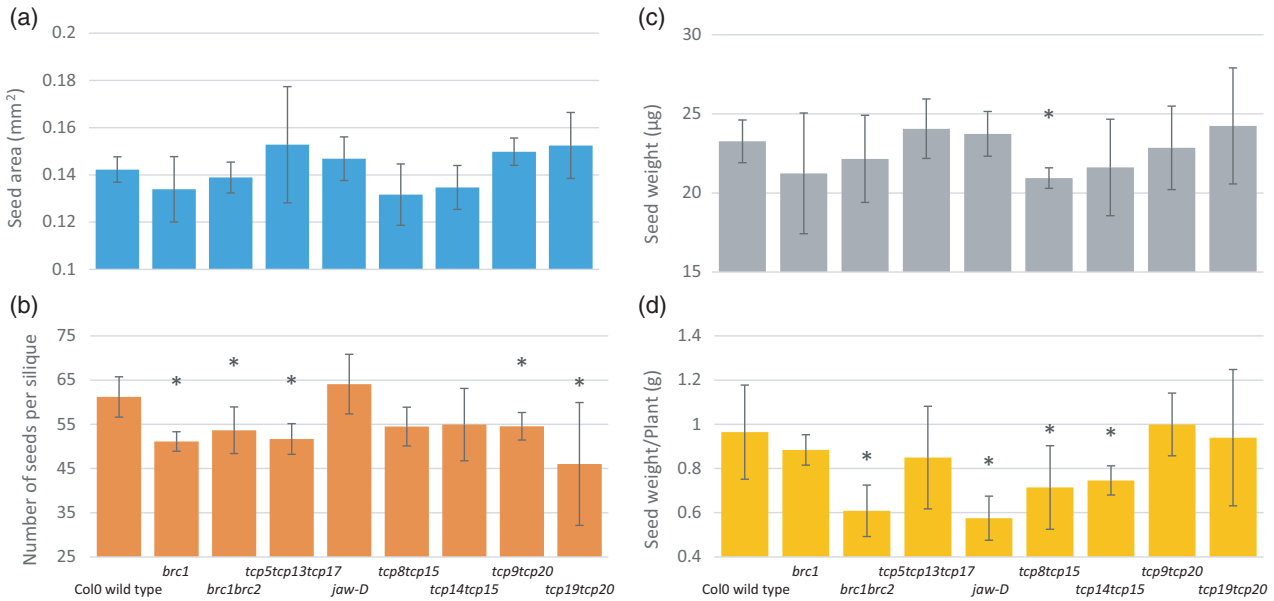

Figure 3. Genotypes showing differences in yield characteristics.
Quantification of yield characteristics such as average seed area (a), average seed number per silique (b), total seed weight per plant and average weight of the individual seed in (c) and (d) respectively. Only genotypes are shown for which statistically significant differences were found compared with wild-type control for at least one of the investigated parameters. Average seed number and seed area were determined on four siliques on five plants per genotype. Statistically significant differences with wild-type (Student's *t*-test, $P < 0.05$) are indicated by an asterisk.

showed a significant difference to Col-0 are presented. We found, as expected, that *brc1* and *brc1brc2* double mutants showed an increase in secondary branches (Aguilar-Martínez *et al.*, 2007). Conversely, several other lines showed a reduction in some aspects of branching, most notably the *jaw-D* (class II TCPs) and *tcp14tcp15* (class I TCPs) mutant lines, having a significant reduction in the number of secondary branches.

Surprisingly, both an increase as well as a decrease in the number of branches has a negative effect on the total seed weight per plant grown under our conditions (*brc1brc2*, *jaw-D*, and *tcp14tcp15* in Figure 3d). We cannot exclude that these genes are also involved in seed characteristics independently from their function in the development of branches. However, this possibility seems unlikely for the *BRANCHED*-like genes as they are reported to be expressed in axillary buds only. Interestingly, the number of secondary branches is not correlated to the number of lateral branches (Figure S5d).

Plants produce fewer branches as a result of a low red to far-red (R:FR) ratio, known as the shade-avoidance response, which can be achieved by high plant density (Casal, 2012). Taking this knowledge into account, we investigated branching under slightly higher plant density in a separate experiment. We grew the plants 6 cm apart, compared with the 9 × 7.5 cm in the initial 'Phenovator' experiment. In general, the number of secondary branches was reduced when the plants were grown at higher density, as nicely exemplified for the Col-0 wild-type plants (Figure 4d–f). As expected, we also found insensitivity of *brc1* for different R:FR ratios (Aguilar-Martínez *et al.*, 2007), validating the experiment's effectiveness (Figure 4d). Interestingly, two other clades of class II TCPs (*tcp5*-likes and *jaw-D* mutants) showed a strong reduction in number of secondary branches grown under higher planting density (Figure 4d–f), a phenotype unnoticed in previous experiments. Additionally and surprisingly, we observed more lateral branches under higher planting density for all investigated lines. Overall, observed phenotypic alterations in the Phenovator experiment could be confirmed and observed effects on secondary branching were enhanced due to the higher plant density, as expected.

DISCUSSION

The aim of this research was to provide a comprehensive overview of differences in developmental, vegetative growth, and seed yield characteristics between a carefully chosen set of *tcp* mutants and wild-type plants. We have developed an approach that describes the growth curve during the vegetative stage of development, using four different biologically meaningful parameters. Variation in these parameters among different *tcp* mutant lines could be clearly represented by a PCA (Figure 1). Interestingly, for all of the genotypes studied, a difference in at least one of the growth equation parameters was observed, which is not surprising as TCPs are involved in different aspects of plant development (reviewed by Martín-Trillo and Cubas, 2010; Uberti Manassero *et al.*, 2013; Nicolas and Cubas,

(a)

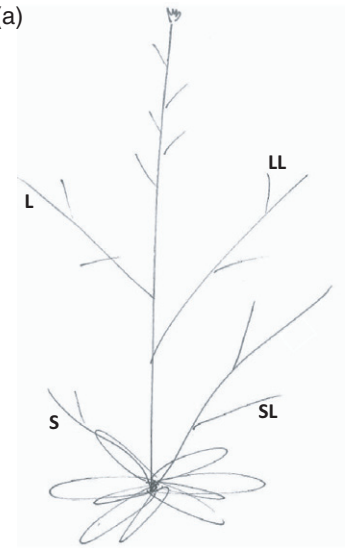

(b)

Experiment 1. Phenovator

Mutant type	S	SL	L	LL	p_S	p_{SL}	p_L	p_{LL}
Col0	4.0	2.3	3.4	1.5				
brc1	7.3	2.9	3.5	1.0	0.00	0.00	0.77	0.19
brc2	4.3	3.1	3.3	1.8	0.57	0.03	0.68	0.41
brc1brc2	9.5	3.8	4.8	1.2	0.00	0.00	0.01	0.69
tcp20tcp22	4.7	1.6	3.7	2.0	0.01	0.21	0.45	0.10
tcp20tcp8	4.0	2.3	4.0	2.1	1.00	0.95	0.10	0.04
tcp8	3.8	2.2	4.0	1.9	0.61	0.48	0.01	0.04
tcp8tcp15	3.8	1.2	3.8	1.4	0.57	0.02	0.36	0.96
tcp14tcp15	2.5	2.3	3.3	1.9	0.00	0.13	0.68	0.33
tcp5tcp13tcp17	3.8	0.8	3.4	1.7	0.35	0.01	1.00	0.66
jaw-D	3.0	0.8	3.7	2.2	0.04	0.00	0.43	0.04

(c)

Experiment 2. Increased plant density

Mutant type	S	SL	L	LL	p_S	p_{SL}	p_L	p_{LL}
Col0	2.8	1.9	5.5	2.6				
brc1	7.0	3.0	5.2	2.3	0.00	0.00	0.11	0.01
brc2	3.5	2.1	5.5	2.6	0.02	0.04	1.00	0.86
brc1brc2	8.4	3.7	6.2	2.1	0.00	0.00	0.01	0.13
tcp20tcp22	2.6	2.0	6.2	2.8	0.45	0.99	0.08	0.00
tcp20tcp8	2.4	2.5	5.7	2.7	0.29	0.34	0.67	0.41
tcp8	3.1	1.9	5.8	2.9	0.30	0.53	0.27	0.02
tcp8tcp15	2.1	1.3	6.2	3.2	0.28	0.02	0.04	0.00
tcp14tcp15	2.2	2.2	5.0	3.5	0.03	0.82	0.01	0.00
tcp5tcp13tcp17	1.3	1.8	6.3	2.8	0.00	0.01	0.00	0.02
jaw-D	0.9	0.2	6.5	3.0	0.00	0.00	0.00	0.00

(d)

Response to increased plant density

Mutant type	p_S	p_{SL}	p_L	p_{LL}
Col0	0.01	0.33	0.00	0.00
brc1	0.62	0.87	0.00	0.00
brc2	0.22	0.54	0.00	0.02
brc1brc2	0.24	0.87	0.00	0.00
tcp20tcp22	0.00	0.72	0.00	0.00
tcp20tcp8	0.00	0.16	0.00	0.46
tcp8	0.00	0.75	0.00	0.00
tcp8tcp15	0.00	0.50	0.00	0.00
tcp14tcp15	0.48	0.67	0.00	0.00
tcp5tcp13tcp17	0.00	0.49	0.00	0.01
jaw-D	0.00	0.00	0.00	0.28

(e)

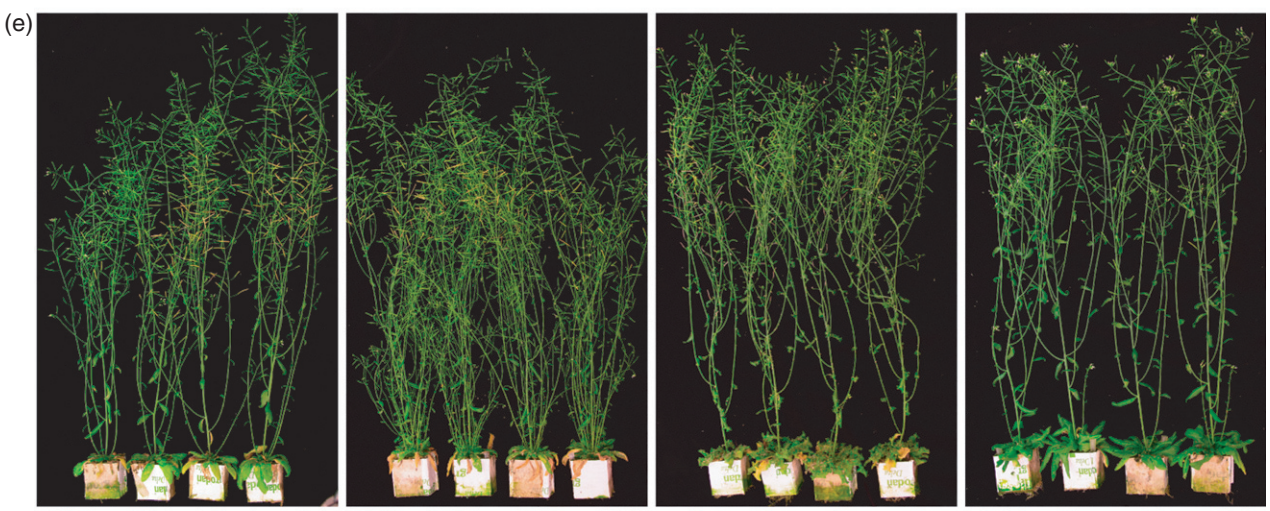

(f)

Figure 4. Branching phenotypes.
(a) Schematic visualization of the position of secondary branches (S), lateral branches (L), branches on secondary branches (SL) and branches on lateral branches (LL).
(b) Branching parameters obtained from plants grown in the 'Phenovator' phenotyping system.
(c) Branching parameters for the same mutants as shown in (b) but grown under higher plant density in a separate 'Increased plant density' experiment. In both (b) and (c) red and green indicate a significant decrease or increase in number of branches respectively, compared with wild-type control, followed by a table with the outcome of Student's *t*-tests ($P < 0.05$, $n = 25$; grey shaded) per branching parameter. Only genotypes are shown for which statistically significant differences were found compared to wild-type control.
(d) Shows the response to the increased planting density per line, red indicates a statistically significant decrease of branching, green a significant increase (Student's *t*-tests, $P < 0.05$) in the 'Increased plant density' experiment compared to the 'Phenovator' experiment.
(e) Pictures of representative plants of the various lines in 'Experiment 2. Increased plant density', showing the observed differences in branching phenotype compared with wild-type control for the *brc1brc2*, *jaw-D* and *tcp5tcp13tcp17* class II TCP mutants.
(f) Zoom-in of the pictures in (e), highlighting the secondary branching phenotypes.

2015, 2016; Danisman, 2016). Next to this, characterising branching parameters and seed yield characteristics on fully mature plants revealed that several *tcp* mutant lines behaved differently compared with wild-type with respect to number and weight of seeds (Figure 3) and the number of branches (Figure 4).

The role of TCP transcription factors in growth regulation during the vegetative stage of plant development

Even though our study does not venture into the cellular level of development, we can speculate on the underlying cellular mechanism causal for the observed differences in

the individual growth equation parameters (β-values) based on whole plant imaging. β_3 for example is supposed to represent the moment a plant enters the rapid growth phase. This moment is typically marked, at the cellular level, by a switch from cell proliferation into cell elongation (Andriankaja *et al.*, 2012). Some well studied class II *tcp* mutants are thought to reside longer in the cell proliferation phase producing more, but often smaller, cells for example *jaw-D* and related *cin* mutants (Nath *et al.*, 2003; Crawford *et al.*, 2004; Challa *et al.*, 2019). In the jaw-D mutant this is represented by a higher β_3 compared with wild-type as it simply takes this mutant longer to reach the phase of rapid and exponential rosette growth. The jaw-D mutant shares its relatively slow progress of growth with a line mutated for the closely related *TCP* genes *TCP5*, *TCP13*, and *TCP17* (*tcp5tcp13tcp17* mutant; Efroni *et al.*, 2008). A delay in leaf and rosette development can also be caused by a reduced speed of cell elongation, a lower β_2, which was indeed observed in the *jaw-D* and the *tcp5tcp13tcp17* triple mutant.

Several genotypes such as *tcp19tcp20tcp22*, *tcp9*, and *tcp20* exhibit a lower β_3 compared with wild-type, suggesting that they enter the cell elongation phase earlier, as was previously shown for *tcp20* (Danisman *et al.*, 2012). The single *tcp9* and the double *tcp9tcp20* mutants showed a cellular phenotype similar to that of *tcp20* (Danisman *et al.*, 2012). In our experiment however, the double *tcp9tcp20* does not show difference in β_3, suggesting that *TCP9* has unique functions and in this is epistatic over *TCP20*. Additionally, several class I mutants show a similar effect on β_3 as the class II *jaw-D* mutant, for example the double mutants *tcp14tcp15* and *tcp8tcp20.*

Focussing on β_1, which represents the maximum of growth, only *brc1brc2* and *tcp8tcp15* have a lower β_1 than wild-type. Several other mutants show a higher β_1, such as the single *branched* mutants as well as *tcp15* and the *tcp14tcp15* double mutant. Molecularly, β_1 is hard to interpret as the final size is influenced by numerous factors other than altered growth speed and timing of rapid growth; for instance, the maximum growth is also dependent on the flowering time, a trait that has not been measured in this study. Additionally, some lines might not have reached their final size during the measurement period.

Next to the growth parameters, we also studied branching patterns. Best studied in this respect are the *branched* mutants that produce more branches than wild-type, most notably the *brc1brc2* double and the *brc1* single mutants (Aguilar-Martínez *et al.*, 2007). In addition, we found that the *jaw-D* and *tcp5tcp13tcp17* (class II), and *tcp14tcp15* (class I) mutant lines showed a significant reduction in the number of secondary branches (Figure 4b). This suggests that next to the *BRANCHED* TCPs, more TCPs are involved in the control of axillary bud outgrowth, either directly by acting in the meristem, or indirectly, for example through changes in sink-source relationships, hormone levels or availability of carbon resources. Promoter GUS fusions of several class II TCPs revealed *TCP3* (a *JAW*-like TCP) and *TCP5* expression in axillary buds (Koyama *et al.*, 2007), enabling cell-autonomous control over axillary bud outgrowth. When grown under higher plant density, significantly fewer branches are observed in *jaw-D*, *tcp5tcp13tcp17* and *tcp14tcp15* mutants and significantly more secondary branches were found in the various *brc* mutants and *tcp20tcp22* (Figure 4c). These effects are most likely related to the altered R:FR light ratio. In *Sorghum bicolor*, the photoreceptor phyB is thought to negatively regulate the *BRC1* homologue *SbTB1* (Kebrom *et al.*, 2010) and a recent study showed that *TCP5*, *TCP13*, and *TCP17* directly upregulate several PHYTOCHROME INTERACTING FACTOR's (PIFs) (Zhou *et al.*, 2017), resembling known interactors of phyB. Additionally, TCP15 activity was shown to be modulated by high light intensities (Viola *et al.*, 2015). Altogether, this leads to the hypothesis that these specific TCPs are involved in light-sensing or signaling and thereby influencing branching architecture of a plant under different light conditions.

TCPs do not show expected redundant behavior for phenotypes tested

The BRANCHED subgroup of TCPs are believed to act redundantly; however, they show striking growth phenotypes. Visualising their rosette growth pattern reveals that both the *brc1* and *brc2* single mutants eventually outgrow Col-0 control plants, although *brc1* grows slower in the first few days of measuring. The *brc1brc2* double mutant conversely grows slower and remains smaller throughout the duration of the measurements (Figure 2b). It must be noted that this observed rosette phenotype could be due to the duration of the measurement and that the *brc1brc2* double mutant might eventually catch up or even outgrow wild-type plants. These observed growth phenotypes suggest that the two Arabidopsis *BRC* genes control each other, possibly through a negative feed-back regulation. This has been shown for *BRC2*, which was upregulated in the *brc1* mutant, possibly compensating for the loss of *BRC1* function (Aguilar-Martínez *et al.*, 2007). Similarly, *BRC1* could be strongly upregulated in the *brc2* mutant, explaining the opposite growth behavior when comparing with the double mutant.

A closer look into the rosette growth of the '*TCP15*-likes' (Figure 1) shows another interesting pattern of single and double mutants. The double mutant *tcp8tcp15* seems almost identical to Col-0 wild-type, whereas both *tcp8* and *tcp15* look vastly different indicating that the combination of *tcp8* and *tcp15* attenuates their individual growth and development effects.

Overall, full redundancy would imply that single mutants show behavior identical to wild-type and only double or higher order mutants would exhibit mutant phenotypes. Based on our data, there are no examples showing true redundancy among the investigated groups of related *TCPs* and their growth phenotypes. The single mutant behavior we have observed would therefore imply only partial redundancy among the analysed members of the *TCP* family of TFs. An example of known partial redundancy is the miR319 regulation of the *JAW-D* TCPs; a single knockout of a gene in this clade produces only mild phenotypes, whereas knocking out the whole clade shows dramatic changes in leaf development (Schommer *et al.*, 2008). This effect can be seen in the higher β_1 for the *tcp10* single mutant, which corresponds to an increase in leaf area as previously observed (Schommer *et al.*, 2008).

Previous research ranked pairs of a number of TCP TFs on their likeliness to be functionally redundant, based on protein sequence, gene expression and Y2H analysis (Danisman *et al.*, 2013). Interestingly, this list showed that the closely related TCP19 and TCP20 ranked high in potential functional overlap, which was confirmed by a detached leaf senescence experiment. Although TCP8 is as closely related to TCP20 as is TCP19 based on sequence similarity, no shared function of TCP8 with TCP20 was found (Danisman *et al.*, 2013). The data presented here show that during rosette development, TCP19 and TCP20 do not seem to share a function in growth (both *tcp20* and *tcp19tcp20* are similarly different from wild-type, independent of the presence or absence of a functional *TCP19* gene), whereas the double mutant *tcp8tcp20* seems to enhance the *tcp20* single mutant phenotype (Figure 1). Further research into the exact molecular function of each TCP protein is necessary to be conclusive on the potential partial functional redundancy.

Two classes of TCPs, showing antagonistic behavior?

Historically, the TCP family of TFs has been divided into two classes based on sequence characteristics (Cubas *et al.*, 1999). Members of these two classes are believed to act antagonistically, either by promoting cell growth and proliferation (class I) or through the repression of these processes (class II) (Martín-Trillo and Cubas, 2010). Whether looking at different β-values in Figure S3(b) or at the distribution of the data points in the PCA plot in Figure 1, one cannot easily identify differences between class I and class II TCPs. This could be due to the nature of our measurements, looking at whole rosette growth as opposed to the cellular level in which the opposite function is observed (Nath *et al.*, 2003; Crawford *et al.*, 2004; Danisman *et al.*, 2012). This notwithstanding, our results question this strict division into two antagonistically functioning classes. Mutants from particular members of class I and class II *TCP* genes show similar changes in specific β-parameters. More comparative research will be necessary to elude either antagonistic or similar behavior. Supporting our data, the *CYCLOIDEA* gene in Antirrhinum is known to both suppress and promote growth of the dorsal petals depending on the developmental stage (Luo *et al.*, 1995).

Next to the growth phenotypes we describe, branching patterns also lack a strict opposite behavior for plant mutagenized in either class I or II TCPs. The increase in branching of *brc1brc2* double mutants would imply that a class I mutant should exhibit fewer branches. This is the case for *tcp14tcp15*, but also the class II mutants *jaw-D* and *tcp5tcp13tcp17* show a decrease in some of the investigated branching parameters. Growing plants with an increase in plant density seemed to increase this effect (Figure 4). This similarity in phenotypes could indicate overlapping functions, or at least similar final phenotypic effects for proteins of both classes, and therefore questions the functional division of the TCP family of TFs solely based on sequence variation.

The link between plant development and final yield

Our study has provided an excellent body of data allowing for a closer look at the effect of unique plant developmental alterations on plant yield under defined environmental conditions. We have collected data on the architecture of the plants, their developmental progress as well as yield characteristics in terms of total seed production. We have confirmed the link between several seed characteristics by correlation analyses (Figure S5a–c) and showed that an increase in number of seeds is negatively correlated with both seed area and seed weight. This negative correlation has been found before (Gnan *et al.*, 2014) and is in line with an earlier proposed model describing a fixed amount of resources allocated to reproduction (Paul-Victor and Turnbull, 2009).

Strikingly, plants that appear to have several significantly different growth parameters (β's) compared with wild-type, such as *jaw-D*, *tcp14tcp15*, and *brc1brc2*, show altered branching patterns or yield characteristics as well. However, a different progression of growth and rosette development (the β parameters) does not necessarily result in differences in yield or branching patterns. Telling examples are the *tcp8* and *tcp15* single mutants, both show a higher β_1, β_2, and β_3 compared with the wild-type, but no differences in seed yield characteristics have been observed. It has previously been reported that inflorescence architecture is of great influence on final seed yield characteristics. For example, prolonged life span of the Arabidopsis inflorescence in a *fruitful* mutant resulted in more seeds (Balanzà *et al.*, 2018). Furthermore, pruning in Arabidopsis led to the development of longer and larger siliques that contained fewer, but bigger seeds (Bennett *et al.*, 2012). This was attributed again to a reallocation of

resources which could also be applicable in the *brc1* and *brc1brc2* mutants. The production of more branches in these mutants reduces the amount of resources left for seed production, resulting in a reduction in seed yield. This does not explain however the reduction in seed production in the *jaw-D*, *tcp5tcp13tcp17*, and *tcp14tcp15* mutants for instance, whose lack of branching could provide additional resources for seed development.

Altogether, this study makes clear that it is indeed challenging to increase and optimize final crop yield by changing the activity of key developmental regulatory genes, such as TCP transcriptions factors. Previous simple classification into activators and repressors of growth appear not to hold and functions were shown to be context and developmental-stage dependent. Furthermore, despite conservation of overall functions for TCP transcription factors, there are various species-specific differences, among others due to species or lineage-specific gene duplications that directly affect possibilities for knowledge transfer from model species to crops.

EXPERIMENTAL PROCEDURES

Plant materials

Information about all lines and genotypes used in this study is shown in Table S1(a). Col-0 wild-type (NASC) was used as control for the T-DNA mutant lines. The Col-0 wild-type used as background for the *ATML1$_{pro}$:TCP5/13-GFP* transformations served as the control for those particular lines (Col-0 'WUR' in Table S1a). *ATML1$_{pro}$:TCP5-GFP* and *ATML1$_{pro}$:TCP13-GFP* lines were previously generated (van Es *et al.*, 2018).

System set-up and plant growing conditions

All lines mentioned in Table S1(a) were grown under long-day conditions (16/8 light/dark cycle at 21°C) on Rockwool and their seeds were harvested simultaneously for use in the large-scale phenotyping experiments. The seeds were sown on wet filter paper and stratified for 2 days at 4°C to ensure uniform germination. After stratification, the seeds were placed on wet Rockwool (www.grodan.com), that was pre-soaked in a nutrient solution designed for Arabidopsis (van Rooijen *et al.*, 2015; Flood *et al.*, 2016). The seeds were placed in the phenotyping system (Phenovator, Flood *et al.*, 2016) at day zero. The Phenovator allows to grow 1440 plants simultaneously in a grid of 24 by 60, placed upon an ebb and flood hydroponic system. The analysis software is unable to distinguish between overlapping plants and therefore only half of the available positions were used, resulting in a planting grid of 9 × 7.5 cm. The grid was divided into 28 plots, in which all 24 genotypes were randomly positioned to prevent a possible positional bias. The plants were grown in the Phenovator under a 16/8 day/night rhythm at a constant temperature of 20°C, relative humidity of 70%, and constant irradiance of 200 μM m^{-2} sec^{-1}.

Measurement schematics

The Phenovator system (Flood *et al.*, 2016) was used to measure two different parameters: PSII operating efficiency (ΦPSII) and near-infrared reflection at 790 nm (NIR). The raw data are provided in Table S2. ΦPSII was measured daily at Zeitgeber (ZT) one, five, eight, 11, and 13. Data obtained through the NIR reflection were used to determine PLA. The wavelength (790 nm) was chosen so that plants could be measured both day and night without disturbing their circadian rhythm. The plants were imaged from day 8 until day 25, until overlapping leaves of neighbouring plants made distinguishing between individual plants impossible. For a detailed overview of the light and measurement regime described above, see Table S1(b).

Subsequently, full-grown plants were phenotyped on their level of branching, total seed set as well as several yield characteristics such as number of seeds per silique, size of seeds, and the seed weight. Phenotyping of branching was done by manually counting the number of lateral shoots and branches on the main inflorescence. Total yield was determined by weighing all the seeds for eight plants per genotype. Seeds size and number per silique was measured for four siliques on five plants per genotype. The seeds were pictured using a set-up designed for imaging seeds and their germination: the 'germinator' (Joosen *et al.*, 2010). We used this software for seed imaging, after which the pictures were analysed by the 'Analyse particles' function in ImageJ, obtaining surface area.

Data handling and pre-processing of growth experiment

Raw data generated by the Phenovator (Table S2) are converted into .csv files with data on the physiological parameters (e.g. ΦPSII or PLA through the NIR images). Non-germinated seeds were identified by a lack of signal in the PAM dataset the 25th day of the experiment. Coordinates in which no signal was observed were removed from both NIR and PAM datasets. The SpATS package (Rodríguez-Álvarez *et al.*, 2016) was used to correct for the observed spatial bias in the PLA dataset.

Creation of a formula to describe the progress of growth for all plants

The PLA time series consisted of 110 data points per coordinate (i.e. individual plant) and was analysed by singular spectral analysis (SSA) using the R-package Rssa (Golyandina *et al.*, 2013). Elementary components (ECs) were retrieved by '*residuals()*'. Based on visual assessment of the ECs growth function (1) was constructed, which consists of two parts: one describing an S-curve, accounting for the actual growth of the plants (Zeide, 1993; Tessmer *et al.*, 2013) and one accounting for the circadian rhythm (Engelmann *et al.*, 1992):

$$f(t) = \underbrace{\left\{\frac{\beta_1}{1 + e^{-\beta_2(t-\beta_3)}}\right\}}_{g(t)} \underbrace{[1 + \beta_4(\sin(2\pi t - \beta_5) - 1)]}_{h(t)} \quad (1)$$

The parameters of function (1) were then estimated by non-linear regression, using the '*nls*' function in R, for each individual coordinate (i.e. individual plant) in the time series. The specific algorithm used was originally introduced as the NL2Sol algorithm (Dennis *et al.*, 1977). Lower and upper bounds that are implemented in the *port* function, and starting values are required. For the parameters in the first part of $f(t)$ in between curly brackets referred, to as $g(t)$, a set of starting values for each of the time series was determined using their basic properties:

$$\beta_1 = \lim_{t\to\infty} g(t) \quad (2a)$$

$$\beta_2 = \frac{g'(0)}{g(0) - g(0)^2/\beta_1} \quad (2b)$$

$$\beta_3 = \frac{\ln(\frac{\beta_1}{g(0)} - 1)}{\beta_2} \quad (2c)$$

Estimates for $\lim_{t\to\infty} g(t)$, $g(0)$, and $g'(0)$ were used to determine starting values of the βs. As the first EC resulting from the SSA is used as an approximation for $g(t)$ as it contributes to $g(t)$ for 99% in terms of covariance. For each of the time series this component is a vector of length 110; EC = $\{EC_1, EC_2, \ldots, EC_{110}\}$, with the corresponding time values as $t = \{t_1, t_2, \ldots, t_{110}\}$.The required approximations are:

$$\lim_{t\to\infty} g(t) \approx \max\{EC\} \quad (3)$$

$$g(0) \approx EC_1 \quad (4)$$

$$g'(0) \approx \frac{EC_5 - EC_1}{t_5 - t_1} \quad (5)$$

The necessary bounds were assessed using the available biological information, such as growth stages of Arabidopsis (Boyes *et al.*, 2001). Note that the exact values of these bounds are not extremely important, as long as they are biologically meaningful and the optimal parameter value lays within the bounds this will ensure that the algorithm converges. For β_1, the natural lower bound is $\beta_{1,lower} = 0$ and the upper bound was set to $\beta_{1,upper} = 3 * \max\{EC\}$ as the plants were measured until 25 days after sowing, which approaches the time a wild-type Arabidopsis plant needs to reach maximum rosette size (Boyes *et al.*, 2001). The measurements started 8 days after sowing and continued for 17 days, so it is unlikely that a plant has already reached the point of most rapid growth (β_3) at time 0 and conversely, 30 days is a safe upper bound, assuming a plant has reached its maximum size almost 40 days after sowing. The parameter β_2 is closely related to β_3 and was inferred by:

$$\beta_2 = \frac{2}{\beta_3 - t_{tang,0}} \quad (6)$$

Here $t_{tang,0}$ is the time coordinate for which the tangent of $g(t)$ at the inflection point intersects the t-axis. The part of the function $g(t)$ left of the inflection point is convex. Therefore, every tangent in that part lies below the function. This, combined with the expectation that $g(0)$ is very small, as the plants just started growing at time 0, implies that $t_{tang,0} \leq 0$. Most of the growth of the plant happens between $\beta_3 - t_{tang,0}$ and $\beta_3 + (\beta_3 - t_{tang,0})$, that is within a time span of $2(\beta_3 - t_{tang,0})$. We assumed $2(\beta_3 - t_{tang,0}) \geq 4$ as it is highly unlikely that most of the growth of the plants happens within 4 days. Combining these bounds with equation (6) yields $\frac{2}{\beta_3} \leq \beta_2 \leq 1$ which allowed us to formulate the following estimations of bounds:

$$0 \leq \beta_1 \leq 3 * \max\{EC\} \quad (7a)$$

$$\frac{1}{15} \leq \beta_2 \leq 1 \quad (7b)$$

$$0 \leq \beta_3 \leq 30 \quad (7c)$$

The second part of $f(t)$, shown in function (1) in between square brackets as $h(t)$, is an oscillatory function with a period of 1 day, describing leaf movement represented by β_4. We assumed a starting value of $\beta_{4,start} = 0.05$. As it is unlikely that the circadian movement of the rosette leaves will result in more than 50% change in area, a reasonable upper bound is therefore $\beta_{4,upper} = 0.5$. The moment the circadian rhythm starts is represented by β_5, i.e. the phase-shift of the oscillation. The range of β_5 is naturally bound between $0 \leq \beta_5 \leq 2*\pi$. The average value of $\beta_{5,start} = \pi$ was chosen. Finally, identification and visualisation of differences between average β-values (Per analysed line; see Table S1) was performed by PCA using *prcomp()* in R, scale set to 'true'. To test whether the differences in the measured variables between the wild-type and mutants are significant, some two-sided *t*-tests were performed at a significance level of 0.2.

Data handling yield characteristics and branching parameters

Yield characteristics were described as mentioned above and several PCA were performed on all measured variables. Again the *prcomp()* command was used to perform this analysis. A single parameter is introduced to capture most of the variance of the four branching parameters, defined as the linear combination given by the first principal component, resulting from the PCA between the four branching parameters. Regression analysis using the *lm()* command was performed to test whether correlations between the variables number, area, and weight exist.

ACKNOWLEDGEMENTS

We would like to thank J. Harbinson and A.E. Prinzenberg for their help in the experimental set-up, initial data analyses and fruitful discussions. We greatly appreciate the members of the PDS research group for their help in setting up the 'Phenovator' experiment and J. Busscher-Lange for her assistance with quantifying the branching phenotypes. W.T. Kruijer recommended the use of the SpATS package. Our work is supported by grants from the Dutch Scientific Organization (NWO); (NWO-JSTP grant 833.13.008), CAPES/NUFFIC (no. 010/07) and CAPES/NUFFIC (no. 033/2012). This research was partly financed through an 'Enabling Technologies Hotel' (ZonMw 435002014).

CONFLICT OF INTEREST

The authors declare no conflict of interest.

SUPPORTING INFORMATION

Additional Supporting Information may be found in the online version of this article.

Figure S1. Regression analysis of positional effects in the experimental set-up.

Figure S2. Designing a growth function based on rosette size measurements over time.

Figure S3. Average values for all four beta parameters.

Figure S4. Comparison of photosynthetic efficiency for the various *tcp* mutants.

Figure S5. Correlation analysis of the seed and branching parameters.

Table S1. Mutant lines and measurement regime used in this study.

Table S2. Raw ΦPSII and NIR data generated by the Phenovator platform.

REFERENCES

Aguilar-Martínez, J.A., Poza-Carrión, C. and Cubas, P. (2007) Arabidopsis BRANCHED1 acts as an integrator of branching signals within axillary buds. *Plant Cell*, **19**, 458–472.

Alonso, J.M., Stepanova, A.N., Leisse, T.J., *et al.* (2003) Genome-Wide Insertional Mutagenesis of *Arabidopsis thaliana*. *Science*, **301**, 653–657.

Aguilar-Martínez, J.A. and Sinha, N. (2013) Analysis of the role of Arabidopsis class I TCP genes AtTCP7, AtTCP8, AtTCP22, and AtTCP23 in leaf development. *Frontiers in plant science*, **4**, 406.

Andriankaja, M., Dhondt, S., De Bodt, S. *et al.* (2012) Exit from proliferation during leaf development in *Arabidopsis thaliana*: a not-so-gradual process. *Dev. Cell*, **22**, 64–78.

Baker, N.R. (2008) Chlorophyll fluorescence: a probe of photosynthesis in vivo. *Annu. Rev. Plant Biol.* **59**, 89–113.

Balanzà, V., Martínez-Fernández, I., Sato, S., Yanofsky, M.F., Kaufmann, K., Angenent, G.C., Bemer, M. and Ferrándiz, C. (2018) Genetic control of meristem arrest and life span in Arabidopsis by a FRUITFULL-APETALA2 pathway. *Nat. Commun.* **9**, 564.

Bennett, E., Roberts, J.A. and Wagstaff, C. (2012) Manipulating resource allocation in plants. *J. Exp. Bot.* **63**, 3391–3400.

Boyes, D.C., Zayed, A.M., Ascenzi, R., McCaskill, A.J., Hoffman, N.E., Davis, K.R. and Görlach, J. (2001) Growth stage-based phenotypic analysis of Arabidopsis: a model for high throughput functional genomics in plants. *Plant Cell*, **13**, 1499–1510.

Busov, V.B., Brunner, A.M. and Strauss, S.H. (2008) Genes for control of plant stature and form. *New Phytol.* **177**, 19.

Cai, G., Yang, Q., Chen, H., Yang, Q., Zhang, C., Fan, C. and Zhou, Y. (2016) Genetic dissection of plant architecture and yield-related traits in *Brassica napus*. *Sci. Rep.* **6**, 1–16.

Casal, J.J. (2012) Shade avoidance. *Arabidopsis Book*, **10**, e0157.

Challa, K.R., Rath, M. and Nath, U. (2019) The CIN-TCP transcription factors promote commitment to differentiation in Arabidopsis leaf pavement cells via both auxin-dependent and independent pathways. *PLoS Genet.* **15**, e1007988.

Crawford, B.C.W., Nath, U., Carpenter, R. and Coen, E.S. (2004) Cincinnata controls both cell differentiation and growth in petal lobes and leaves of *Antirrhinum*. *Plant Physiol.* **135**, 244–253.

Cubas, P., Lauter, N., Doebley, J. and Coen, E. (1999) The TCP domain: a motif found in proteins regulating plant growth and development. *Plant J.* **18**, 215–222.

Danisman, S. (2016) TCP transcription factors at the interface between environmental challenges and the plant's growth responses. *Front. Plant Sci.* **7**, 1–13.

Danisman, S., van der Wal, F., Dhondt, S. *et al.* (2012) Arabidopsis class I and class II TCP transcription factors regulate jasmonic acid metabolism and leaf development antagonistically. *Plant Physiol.* **159**, 1511–1523.

Danisman, S., Van Dijk, A.D.J., Bimbo, A., Van Der Wal, F., Hennig, L., De Folter, S., Angenent, G.C. and Immink, R.G.H. (2013) Analysis of functional redundancies within the Arabidopsis TCP transcription factor family. *J. Exp. Bot.* **64**, 5673–5685.

Dennis, J.E., Gay, D.M. and Welsch, R.E. (1977) An adaptive nonlinear least square algorithm. *ACM Trans. Math. Softw.* **7**, 348–368.

Doebley, J., Stec, A. and Gustus, C. (1995) teosinte branched1 and the origin of maize: evidence for epistasis and the evolution of dominance. *Genetics*, **141**, 333–346.

Doebley, J., Stec, A. and Hubbard, L. (1997) The evolution of apical dominance in maize. *Nature*, **386**, 485–488.

Efroni, I., Blum, E., Goldshmidt, A. and Eshed, Y. (2008) A protracted and dynamic maturation schedule underlies Arabidopsis leaf development. *Plant Cell*, **20**, 2293–2306.

Engelmann, W., Simon, K. and Phen, C.J. (1992) Leaf movement rhythm in *A. thaliana*. *Z. Naturforsch.*, **47**, 925–928.

van Es, S.W., Silveira, S.R., Rocha, D.I., Bimbo, A., Martinelli, A.P., Dornelas, M.C., Angenent, G.C. and Immink, R.G. (2018) Novel functions of the Arabidopsis transcription factor TCP5 in petal development and ethylene biosynthesis. *Plant J.* **94**, 867–879.

Flood, P.J., Kruijer, W., Schnabel, S.K., van der Schoor, R., Jalink, H., Snel, J.F.H., Harbinson, J. and Aarts, M.G.M. (2016) Phenomics for photosynthesis, growth and reflectance in *Arabidopsis thaliana* reveals circadian and long-term fluctuations in heritability. *Plant Methods*, **12**, 14.

Genty, B., Briantais, J.M. and Baker, N.R. (1989) The relationship between the quantum yield of photosynthetic electron transport and quenching of chlorophyll fluorescence. *Biochim. Biophys. Acta Gen. Subj.* **990**, 87–92.

Gnan, S., Priest, A. and Kover, P.X. (2014) The genetic basis of natural variation in seed size and seed number and their trade-off using *Arabidopsis thaliana* magic lines. *Genetics*, **198**, 1751–1758.

Golyandina, N., Korobeynikov, A., Shlemov, A. and Usevich, K. (2013) Multivariate and 2D extensions of singular spectrum analysis with the Rssa package. *J. Stat. Softw.* **67**, 1–78.

Joosen, R.V.L., Kodde, J., Willems, L.A.J., Ligterink, W., Van Der Plas, L.H.W. and Hilhorst, H.W.M. (2010) Germinator: a software package for high-throughput scoring and curve fitting of Arabidopsis seed germination. *Plant J.* **62**, 148–159.

Kebrom, T.H., Brutnell, T.P. and Finlayson, S.A. (2010) Suppression of *Sorghum* axillary bud outgrowth by shade, phyB and defoliation signalling pathways. *Plant Cell Environ.* **33**, 48–58.

Kieffer, M., Master, V., Waites, R. and Davies, B. (2011) TCP14 and TCP15 affect internode length and leaf shape in Arabidopsis. *Plant J.* **68**, 147–158.

Koyama, T., Furutani, M., Tasaka, M. and Ohme-Takagi, M. (2007) TCP transcription factors control the morphology of shoot lateral organs via negative regulation of the expression of boundary-specific genes in Arabidopsis. *Plant Cell*, **19**, 473–484.

Leister, D., Varotto, C., Pesaresi, P., Niwergall, A. and Salamini, F. (1999) Large-scale evaluation of plant growth in *Arabidopsis thaliana* by non-invasive image analysis. *Plant Physiol. Biochem.* **37**, 671–678.

Li, C., Potuschak, T., Colón-Carmona, A., Gutiérrez, R.A. and Doerner, P. (2005) Arabidopsis TCP20 links regulation of growth and cell division control pathways. *Proc. Natl Acad. Sci. USA*, **102**, 12978–12983.

Luo, D., Carpenter, R., Vincent, C., Copsey, L. and Coen, E. (1995) Origin of floral asymmetry in Antirrhinum. *Nature*, **383**, 794–799.

Martín-Trillo, M. and Cubas, P. (2010) TCP genes: a family snapshot ten years later. *Trends Plant Sci.* **15**, 31–39.

Nath, U., Crawford, B.C.W., Carpenter, R. and Coen, E. (2003) Genetic control of surface curvature. *Science*, **299**, 1404–1407.

Nicolas, M. and Cubas, P. (2015) Plant Transcription Factors. In *The Role of TCP Transcription Factors in Shaping Flower Structure, Leaf Morphology, and Plant Architecture*. (González, D., ed). Amsterdam, The Netherlands: Elsevier Inc.

Nicolas, M. and Cubas, P. (2016) TCP factors: new kids on the signaling block. *Curr. Opin. Plant Biol.* **33**, 33–41.

Ori, N., Cohen, A.R., Etzioni, A., *et al.* (2007) Regulation of LANCEOLATE by miR319 is required for compound-leaf development in tomato. *Nat. Genet.* **39**, 787–791.

Palatnik, J.F., Allen, E., Wu, X.L., Schommer, C., Schwab, R., Carrington, J.C. and Weigel, D. (2003) Control of leaf morphogenesis by microRNAs. *Nature*, **425**, 257–263.

Paul-Victor, C. and Turnbull, L.A. (2009) The effect of growth conditions on the seed size/number trade-off. *PLoS ONE*, **4**, e6917.

Rodríguez-Álvarez, M.X., Boer, M.P., van, Eeuwijk, F.A. and Eilers, P.H.C. (2016) Spatial Models for Field Trials. 1–39. http://arxiv.org/abs/1607.08255

van Rooijen, R., Aarts, M.G.M. and Harbinson, J. (2015) Natural genetic variation for acclimation of photosynthetic light use efficiency to growth irradiance in *Arabidopsis thaliana*. *Plant Physiol.* **167**, 1412–1429.

Schommer, C., Palatnik, J.F., Aggarwal, P., Chételat, A., Cubas, P., Farmer, E.E., Nath, U. and Weigel, D. (2008) Control of jasmonate biosynthesis and senescence by miR319 targets. *PLoS Biol.* **6**, 1991–2001.

Takeda, T., Suwa, Y., Suzuki, M., Kitano, H., Ueguchi-Tanaka, M., Ashikari, M., Matsuoka, M. and Ueguchi, C. (2003) The OsTB1 gene negatively regulates lateral branching in rice. *Plant J.* **33**, 513–520.

Tessmer, O.L., Jiao, Y., Cruz, J.A., Kramer, D.M. and Chen, J. (2013) Functional approach to high-throughput plant growth analysis. *BMC Syst. Biol.* **7**, 1–13.

Uberti Manassero, N.G., Viola, I.L., Welchen, E. and Gonzalez, D.H. (2013) TCP transcription factors: architectures of plant form. *Biomol. Concepts*, **4**, 111–127.

Velazco, J.G., Rodríguez-Álvarez, M.X., Boer, M.P., Jordan, D.R., Eilers, P.H.C., Malosetti, M. and van Eeuwijk, F.A. (2017) Modelling spatial trends in *Sorghum* breeding field trials using a two-dimensional P-spline mixed model. *Theor. Appl. Genet.* **130**, 1375–1392.

Viola, I.L., Camoirano, A. and Gonzalez, D.H. (2015) Redox-Dependent Modulation of Anthocyanin Biosynthesis by the TCP Transcription Factor TCP15 during Exposure to High Light Intensity Conditions in Arabidopsis. *Plant Physiol.* **170**, 74–85.

Zeide, B. (1993) Analysis of growth equations. *For. Sci.* **39**, 594–616.

Zhou, Y., Zhang, D., An, J., Yin, H., Fang, S., Chu, J., Zhao, Y. and Li, J. (2017) TCP transcription factors regulate shade avoidance via directly mediating the expression of both PHYTOCHROME INTERACTING FACTORs and auxin biosynthetic genes. *Plant Physiol.* **176**, 1850–1861.